Inside-Out Planet Formation

Abstract: The compact multi-transiting planet systems discovered by *Kepler* challenge planet formation theory. Formation *in situ* from disks with radial mass surface density, Σ, profiles similar to the minimum mass solar nebula (MMSN) but boosted in normalization by factors $\gtrsim 10$ has been suggested. We propose that a more natural way to create these planets in the inner disk is formation sequentially from the inside-out via creation of successive gravitationally unstable rings fed from a continuous stream of small (~cm-m size) "pebbles", drifting inwards via gas drag. Pebbles collect at the pressure maximum associated with the transition from a magneto-rotational instability (MRI)-inactive ("dead zone") region to an inner MRI-active zone. A pebble ring builds up until it either becomes gravitationally unstable to form an $\sim 1\text{-}10 M_\oplus$ planet directly or induces gradual planet formation via core accretion. The planet may undergo Type I migration into the active region, allowing a new pebble ring and planet to form behind it. Alternatively if migration is inefficient, the planet may continue to accrete from the disk until it becomes massive enough to isolate itself from the accretion flow. A variety of densities may result depending on the relative importance of residual gas accretion as the planet approaches its isolation mass. The process can repeat with a new pebble ring gathering at the new pressure maximum associated with the retreating dead zone boundary. Our simple theoretical model for this scenario of inside-out planet formation yields planetary masses, relative mass scalings with orbital radius, and minimum orbital separations consistent with those seen by *Kepler*. It provides an explanation of how massive planets can form with tightly-packed system architectures, starting from typical protoplanetary disk properties.

Jonathan C. Tan
Sourav Chatterjee
(University of Florida)

UF | Astronomy

Kepler has found many *systems with tightly-packed inner planets* (STIPs), with closely-spaced ~1-10 Earth-mass planets on well-aligned orbits. There are about 250, 84, 26, and 8 systems with 2, 3, 4, and 5 or more planets in the latest data release from Kepler (Batalha et al. 2013). Most of these planets have orbital periods <100 day. The figure shows systems with 3+ planets (from Fabrycky et al. 2012). Planet radii are to scale and colored by decreasing size in each system: red, orange, green, light blue, dark blue, and grey. These systems also have low (<~3 degree) inclination dispersion (Fang & Margot 2012).
Compact architecture and low inclination dispersion suggest lack of strong dynamical encounters for these planets. They almost certainly formed from gaseous disks, enriched in solids.

A scenario of planet formation in the outer disk followed by subsequent migration to the inner region has been proposed by, e.g. Kley & Nelson (2012). However, this tends to produce orbits trapped near low-order mean motion resonances, which are not a particular feature of the observed STIPs. Alternatively, Hansen & Murray (2012, 2013) proposed this concentration (>~20M$_\oplus$ inside 1AU) is achieved via migration of small bodies to form an inner enriched disk. They then considered a standard model of planet formation via oligarchic growth from such a disk (see also Chiang & Laughlin 2013). Here we consider a model involving simultaneous enrichment and formation.

P (days)
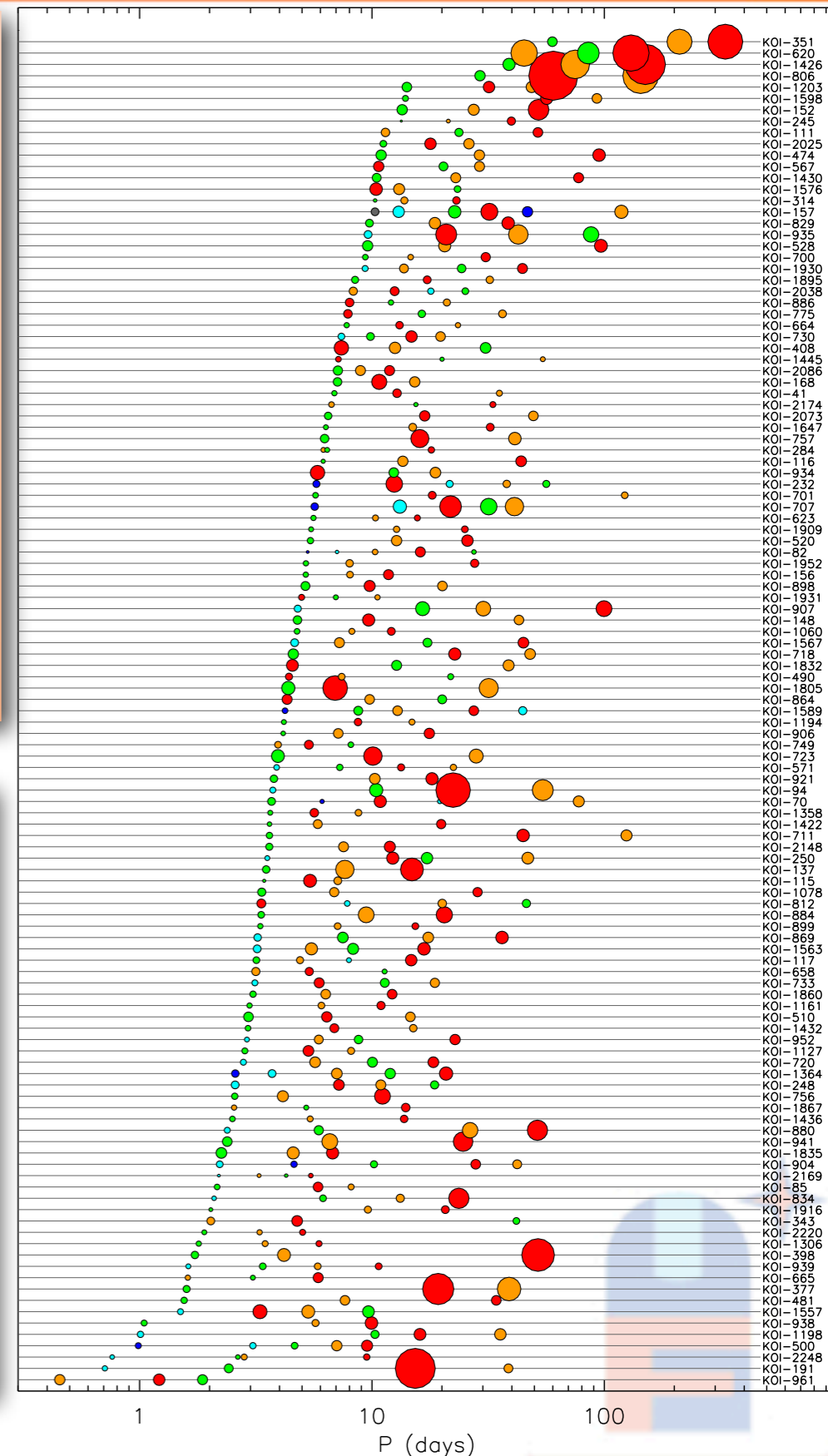
2. A model for *in situ* formation near the star


(i) dead zone — MRI zone — pebble drift
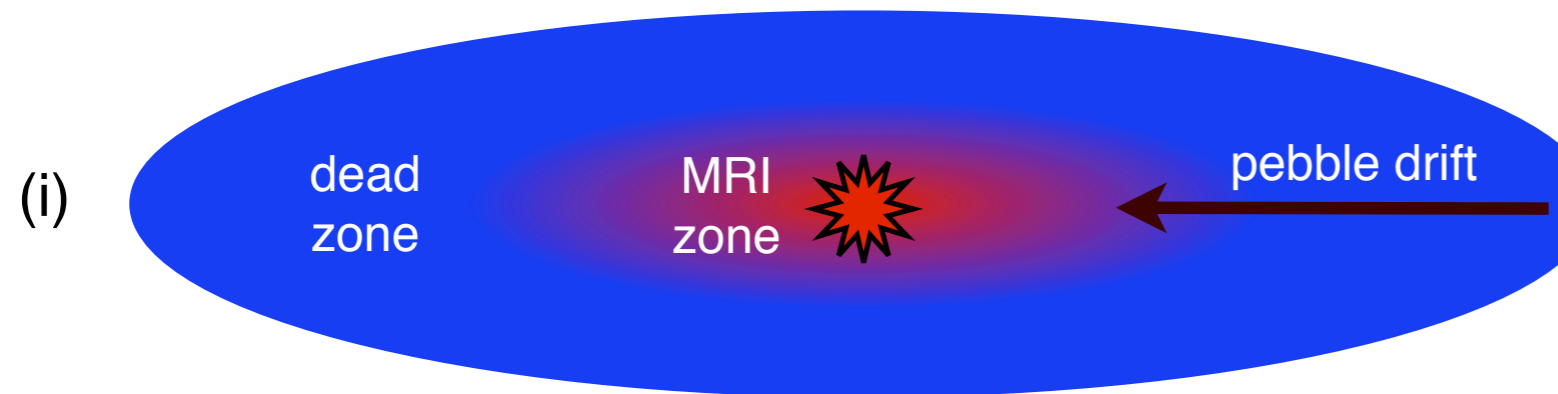
Rapid radial drift of cm to m-sized "pebbles" via gas drag. They collect at the pressure maximum near the dead zone (DZ) inner boundary (IB), likely first set by thermal ionization of alkali metals at ~1200K.

(ii) pebble ring forms at P max
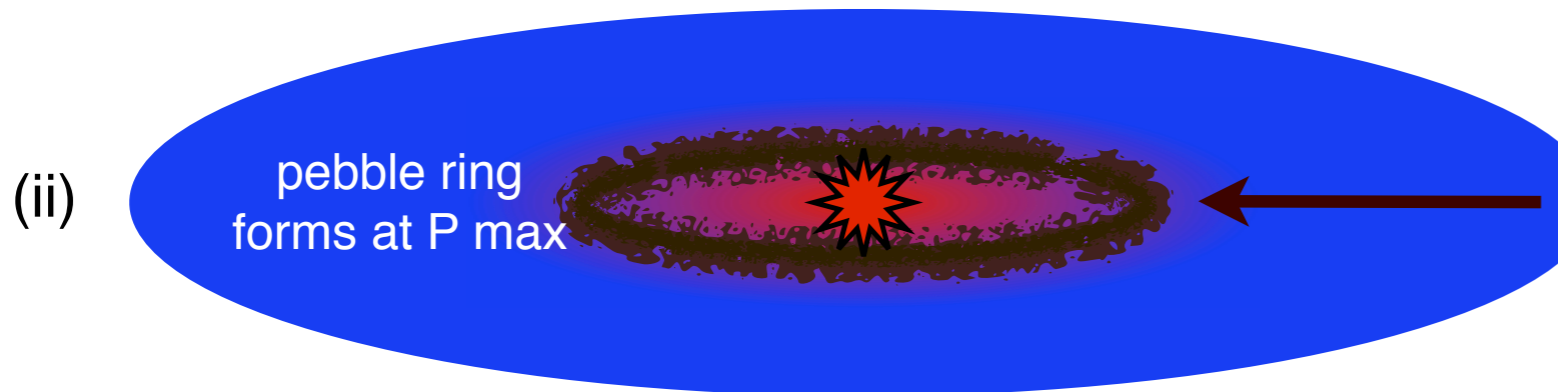
Pebbles concentrate in a relatively narrow ring, and begin to dominate the local gas mass surface density in the disk, $\Sigma_p > \Sigma_g$, eventually by factors of ~10.

(iii) planet formation
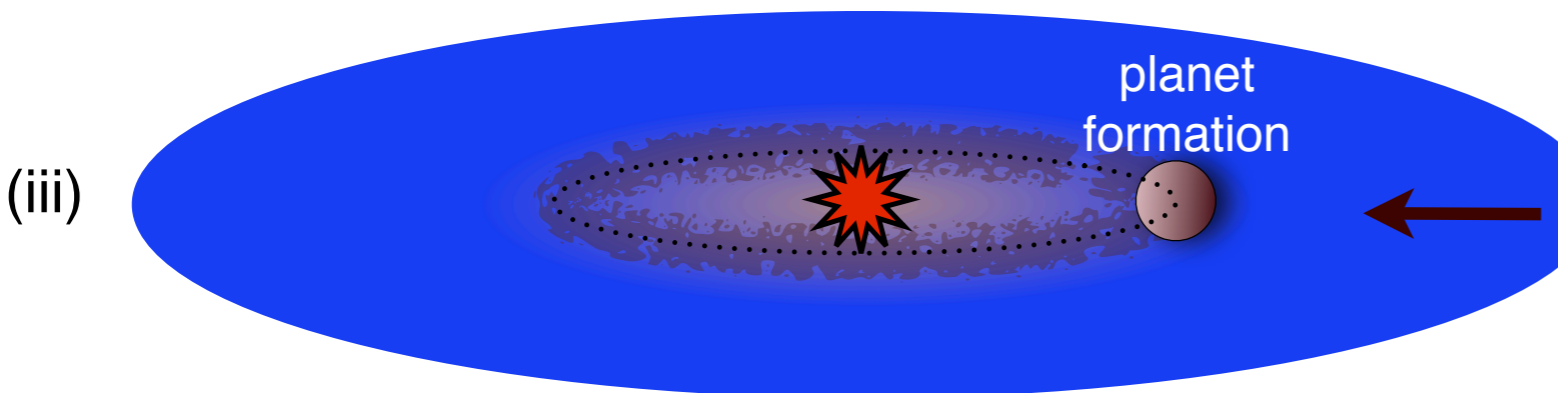
A planet forms from the pebble ring, perhaps via gravitational instability. It may grow to then clear a gap in the gas disk, leading to viscous clearing of the inner disk. Or it may (Type I) migrate inwards.

(iv) dead zone retreat
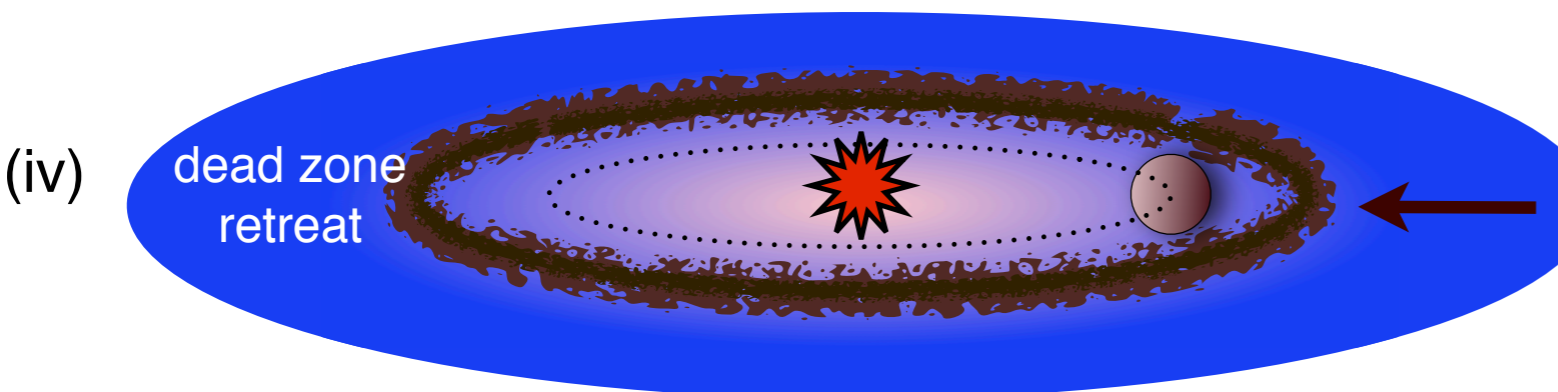
With reduced extinction from the inner disk, the dead zone inner boundary retreats outwards and the process repeats. Or, for the migration scenario, a new ring and planet form at the fixed DZIB.

UF | Astronomy

3. Radial drift of pebbles to the dead zone inner boundary

Pebbles are created by dust grain coagulation in the outer disk. Then...

Once created, gas drag drives pebbles inwards with radial drift velocity v_r, depending on their size and disk pressure profile $P = P_0(r/r_0)^{-k_P}$ via

$$\frac{v_r}{v_K} = \frac{-k_P(c_s/v_K)^2}{\tau_{\text{fric}} + \tau_{\text{fric}}^{-1}}$$

(e.g., Armitage 2007) where c_s is disk midplane sound speed, v_K is Keplerian speed and $\tau_{\text{fric}} \equiv \Omega_K t_{\text{fric}}$ is pebble stopping time, where $\Omega_K = (GM/r^3)^{1/2}$ and t_{fric} is the frictional timescale.

The drift time is short! (evaluating for a standard Shakura-Sunyaev α-disk model)

$$t_{\text{drift}} \equiv \frac{r}{|v_{r,p}|}$$

$$= \frac{2\pi^{2/5}}{3^{1/5} f_\tau k_P} \left(\frac{\mu}{\gamma k_B}\right)^{4/5} \left(\frac{\kappa}{\sigma_{\text{SB}}}\right)^{-1/5} \alpha^{1/5}$$

$$\times (Gm_*)^{1/5}(f_r \dot{m})^{-2/5} r^{7/5}$$

$$\rightarrow 43.9 f_\tau^{-1} \gamma_{1.4}^{-4/5} \kappa_{10}^{-1/5} \alpha_{-3}^{1/5} m_{*,1}^{1/5} (f_r \dot{m}_{-9})^{-2/5} r_{\text{AU}}^{7/5} \text{ yr}$$

A pressure maximum is expected at the inner dead zone boundary:

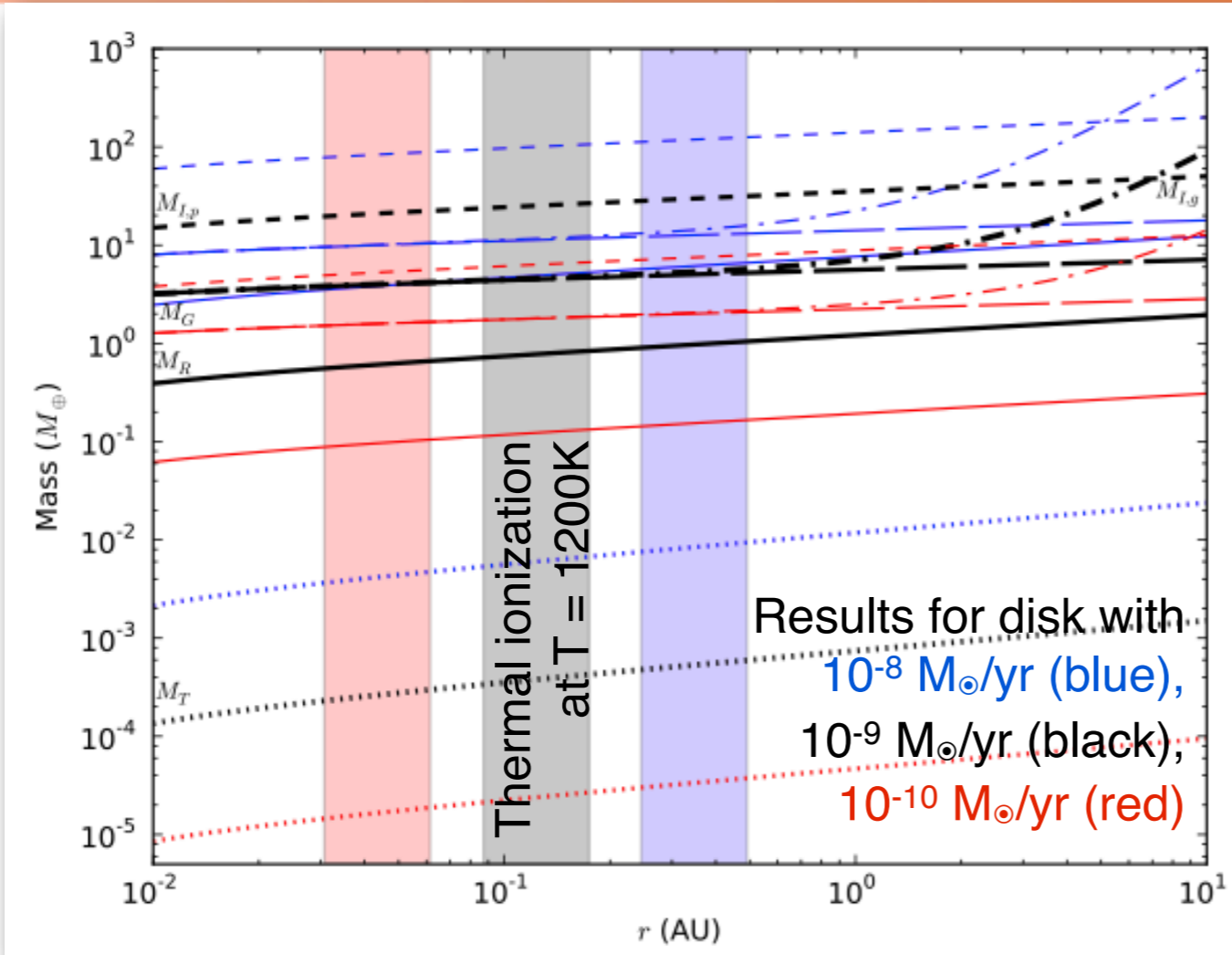For a steady, thin, active accretion disk the midplane pressure at radius $r \equiv r_{\text{AU}} \text{AU}$ is

$$P = \frac{2^{1/2}}{3^{11/10} \pi^{4/5}} \left(\frac{\mu}{k_B}\right)^{2/5} \gamma^{-7/5} \left(\frac{\kappa}{\sigma_{\text{SB}}}\right)^{-1/10} \alpha^{-9/10}$$

$$\times (Gm_*)^{17/20}(f_r \dot{m})^{4/5} r^{-51/20},$$

$$P/k_B \rightarrow 1.22 \times 10^{16} \gamma_{1.4}^{-7/5} \kappa_{10}^{-1/10} \alpha_{-3}^{-9/10}$$

$$\times m_{*,1}^{17/20}(f_r \dot{m}_{-9})^{4/5} r_{\text{AU}}^{-51/20} \text{ K cm}^{-3}$$

$P \propto \alpha^{-9/10}$, so as α rapidly increases on leaving the inner dead zone boundary, midplane pressure decreases almost as rapidly. This analytic expectation of a pressure maximum near the inner dead zone boundary is seen in the simulations of Dzyurkevich et al. (2010).

So pebbles will collect at this boundary.

4. Mass scales of planet formation

Thermal ionization at T = 1200K

Results for disk with
10⁻⁸ M⊙/yr (blue),
10⁻⁹ M⊙/yr (black),
10⁻¹⁰ M⊙/yr (red)

Various processes can set masses of planets forming from the pebble-dominated ring:

1. Toomre Mass, M_T [assume vel. disp. $\sim v_r(r_0)$; $Q \sim 1$]
2. Ring Mass, M_R [if most of the ring accreted to 1 planet]
3. Gap-opening Mass, M_G [fraction $\phi_G = 0.3$ (Zhu et al. 2013) of viscous-thermal criterion; note strong dependence on α]
4. Isolation Mass in gas, $M_{I,g}$, or pebble-dominated, $M_{I,p}$, disk [assuming planet sweeps up material out to $\phi_H(\sim 3$; Lissauer 1987) Hill radii (R_H); isolation may also be achieved by pebble trapping at a larger radius due to dead zone retreat]

$$M_T \equiv \Sigma_p \lambda_T^2 = \frac{\pi \phi_\sigma^3 k_P^3 Q c_s^6 r^3}{2 G^3 m_*^2}$$

$$= \frac{3^{3/5}}{2^4 \pi^{1/5}} \phi_\sigma^3 k_P^3 Q \left(\frac{\mu}{\gamma k_B}\right)^{-12/5} \left(\frac{\kappa}{\sigma_{SB}}\right)^{3/5} \alpha^{-3/5}$$

$$\times G^{-21/10} m_*^{-11/10} (f_r \dot{m})^{6/5} r^{3/10}$$

$$\to 7.60 \times 10^{-4} \phi_{\sigma,0.3}^3 Q \gamma_{1.4}^{12/5} \kappa_{10}^{3/5} \alpha_{-3}^{-3/5}$$

$$\times m_{*,1}^{-11/10} (f_r \dot{m}_{-9})^{6/5} r_{AU}^{3/10} M_\oplus.$$

$$M_R \equiv 2\pi r \lambda_T \Sigma_p = 4\pi r \phi_\sigma^2 \frac{|v_{r,p}|^2}{G} = \frac{\pi \phi_\sigma^2 k_P^2 r^2 c_s^4}{G^2 m_*}$$

$$= \frac{3^{2/5} \pi^{1/5}}{2^2} \phi_\sigma^2 k_P^2 \left(\frac{\mu}{\gamma k_B}\right)^{-8/5} \left(\frac{\kappa}{\sigma_{SB}}\right)^{2/5} \alpha^{-2/5}$$

$$\times G^{-7/5} m_*^{-2/5} (f_r \dot{m})^{4/5} r^{1/5}$$

$$\to 1.23 \phi_{\sigma,0.3}^2 \gamma_{1.4}^{8/5} \kappa_{10}^{2/5} \alpha_{-3}^{-2/5} m_{*,1}^{-2/5} (f_r \dot{m}_{-9})^{4/5} r_{AU}^{1/5} M_\oplus$$

$$M_G = \frac{\phi_G 40 \nu m_*}{r^2 \Omega_K}$$

$$= 20 \frac{3^{1/5}}{\pi^{2/5}} \phi_G \left(\frac{\mu}{\gamma k_B}\right)^{-4/5} \left(\frac{\kappa}{\sigma_{SB}}\right)^{1/5}$$

$$\times \alpha^{4/5} G^{-7/10} m_*^{3/10} (f_r \dot{m})^{2/5} r^{1/10}$$

$$\to 5.67 \phi_{G,0.3} \gamma_{1.4}^{4/5} \kappa_{10}^{1/5} \alpha_{-3}^{4/5} m_{*,1}^{3/10} (f_r \dot{m}_{-9})^{2/5} r_{AU}^{1/10} M_\oplus$$

$$M_{I,g} = \max(M_R, M_G) + dM_g$$
$$dM_g = 2\pi r \phi_{H,g} R_H \Sigma_g$$
$$= 2\pi r^2 \phi_{H,g} (M_{pl}/(3m_*))^{1/3} \Sigma_g$$

$$M_{I,p} = \frac{1}{2^{3/2} 3^{1/5} \pi^{3/5}} \left(\frac{\phi_{H,p} \phi_\sigma k_P}{Q}\right)^{3/2} \left(\frac{\mu}{\gamma k_B}\right)^{-6/5}$$

$$\times \left(\frac{\kappa}{\sigma_{SB}}\right)^{3/10} \alpha^{-3/10} G^{-21/20} m_*^{-1/20} (f_r \dot{m})^{3/5} r^{3/20}$$

$$\to 35.7 \left(\frac{\phi_{H,p,3} \phi_{\sigma,0.3}}{Q}\right)^{3/2} \gamma_{1.4}^{6/5} \kappa_{10}^{3/10} \alpha_{-3}^{-3/10} m_{*,1}^{-1/20}$$

$$\times (f_r \dot{m}_{-9})^{3/5} r_{AU}^{3/20} M_\oplus,$$
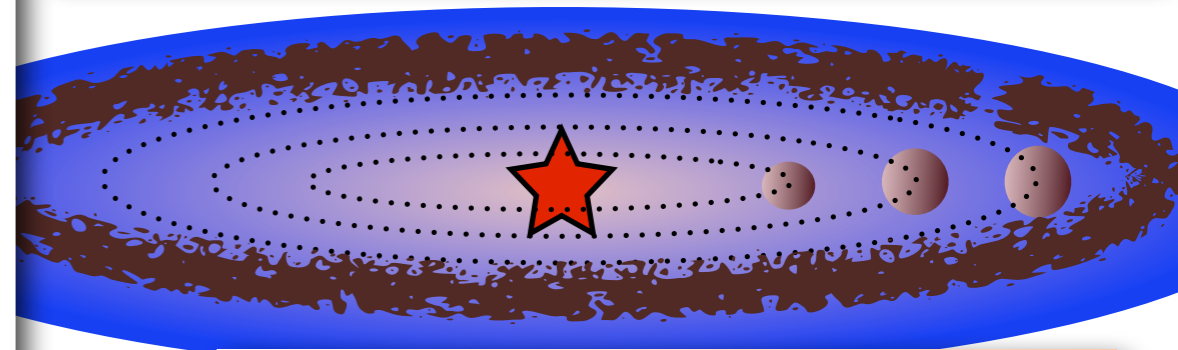
5. Subsequent planet formation

After gap opening by the first planet, protostellar X-ray ionization will penetrate further and the inner boundary of the dead zone will tend to move outwards, by at least $\phi_H \sim 3R_H$, i.e. at least several Hill radii of the already-formed planet.

A new pressure maximum will be established and thus a new pebble ring can form, as long as the supply of pebbles from the outer disk continues. The mass of solids available in the disk out to radius r_1 is:

$$M_s(< r_1) = \int^{r_1} f_s 2\pi r \Sigma_g dr$$

$$= \frac{20\pi^{2/5}}{3^{6/5}7} f_s \left(\frac{\mu}{\gamma k_B}\right)^{4/5} \left(\frac{\kappa}{\sigma_{\rm SB}}\right)^{-1/5} \alpha^{-4/5}$$

$$\times (Gm_*)^{1/5} \dot{m}^{3/5} r_1^{7/5} \qquad (30)$$

$$\to 0.178 f_{s,-2} \gamma_{1.4}^{-4/5} \kappa_{10}^{1/5} \alpha_{-3}^{-4/5} m_{*,1}^{1/5} \dot{m}_{-9}^{3/5} r_{1,\rm AU}^{7/5} \ M_{\oplus}$$

Assuming the first planet forms with mass $M_R = \epsilon_p M_s(< r_1)$ with efficiency $\epsilon_p = 0.5$, we estimate the radius r_1 that becomes depleted of pebbles:

$$r_1 = \left(\frac{7}{5}\right)^{5/7} \frac{3^{8/7}}{2^{20/7}\pi^{1/7}} \frac{(\phi_\sigma k_P)^{10/7}}{(f_s \epsilon_p)^{5/7}} \left(\frac{\mu}{\gamma k_B}\right)^{-12/7} \left(\frac{\kappa}{\sigma_{\rm SB}}\right)^{3/7}$$

$$\times \alpha^{2/7} G^{-8/7} m_*^{-3/7} \dot{m}^{1/7} r_0^{1/7}$$

$$\to 6.55 \frac{\phi_{\sigma,0.3}^{10/7} \gamma_{1.4}^{12/7} \kappa_{10}^{3/7}}{(f_{s,0.01}\epsilon_{p,0.5})^{5/7}} \alpha_{-3}^{2/7} m_{*,1}^{-3/7} \dot{m}_{-9}^{1/7} r_{0,\rm AU}^{1/7} \ {\rm AU}.$$

A large region of the outer disk, out to a few x 10AU is needed to supply enough pebbles to make STIPs with several planets.

Another possible scenario for subsequent planet formation involves inward Type I migration of the planet from the dead zone inner boundary, followed by new ring and planet formation at this same location.

UF | Astronomy

6. Comparison of mass scales with Kepler systems
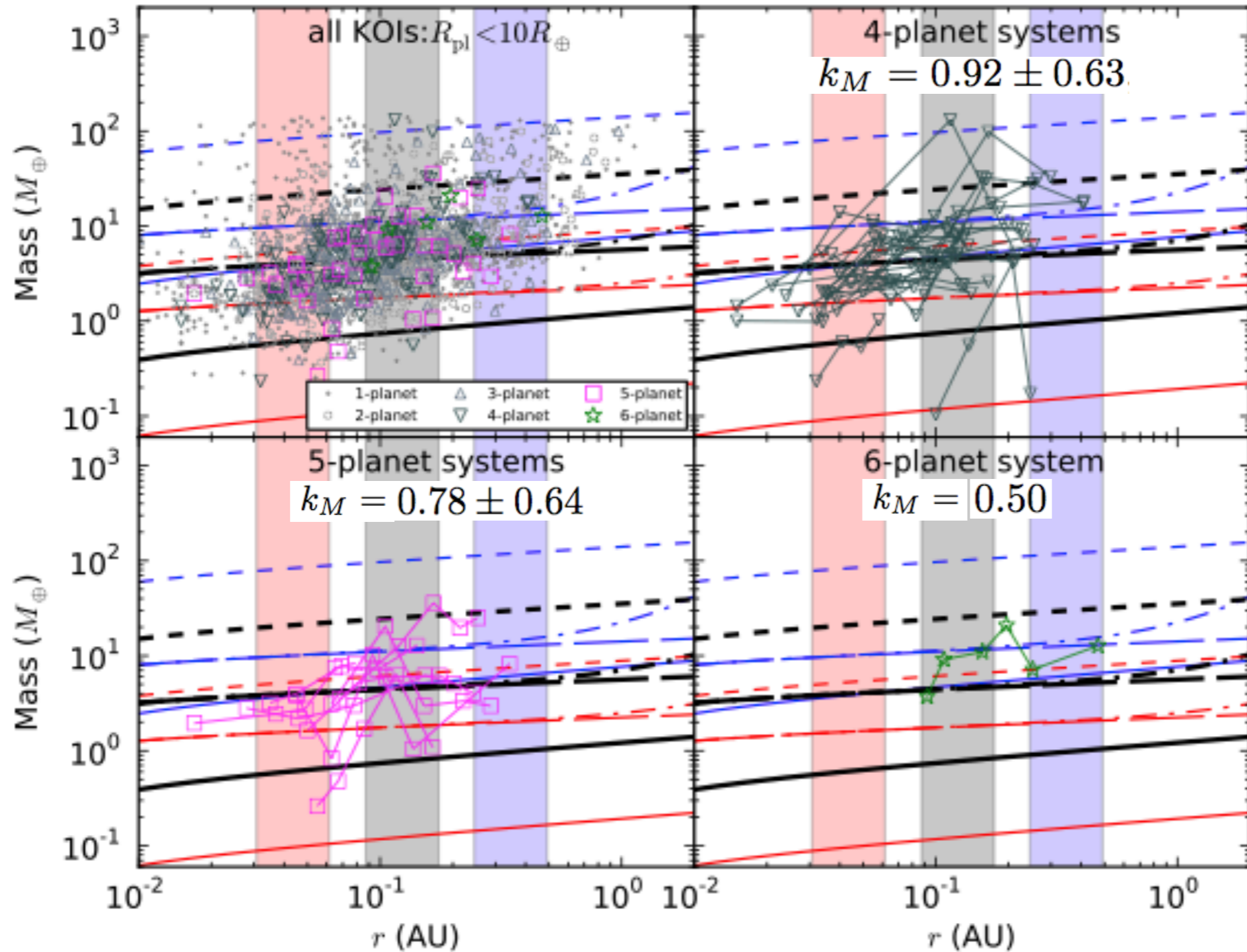
The masses of the observed planets are consistent with the fiducial model predictions assuming isolation in a gas-dominated disk, i.e. after the pebble-dominated ring has been accreted to the planet. Describing the planet mass dependence on radius as

$$M_{\rm pl} \propto r^{k_M}$$

then for $M_{\rm pl} \approx M_{\rm I,g} \approx M_G$, we have $k_M \approx 0.1$ (for $r < 1$AU), approximately consistent with the observed systems.

Mass scale lines as in figure in slide 4. (a) Top-left: planets with $R < 10 R_\oplus$ are shown from Batalha et al. (2013) (16-month data release). (b) Top-right: Only 4-planet systems shown. (c) Bottom-left: Only 5-planet systems shown. (d) Bottom-right: Only the 6-planet system shown. Note, planet masses are rough estimates from a simple scaling with radius ($M_{\rm pl} = M_\oplus (R_{\rm pl}/R_\oplus)_\oplus^{2.06}$, Lissauer et al. 2011).

7. Masses of the TTV systems

The masses shown in slide 6 are derived from observed sizes and so are quite approximate. A much smaller number of systems have direct mass measurements via transit timing variations (TTV):
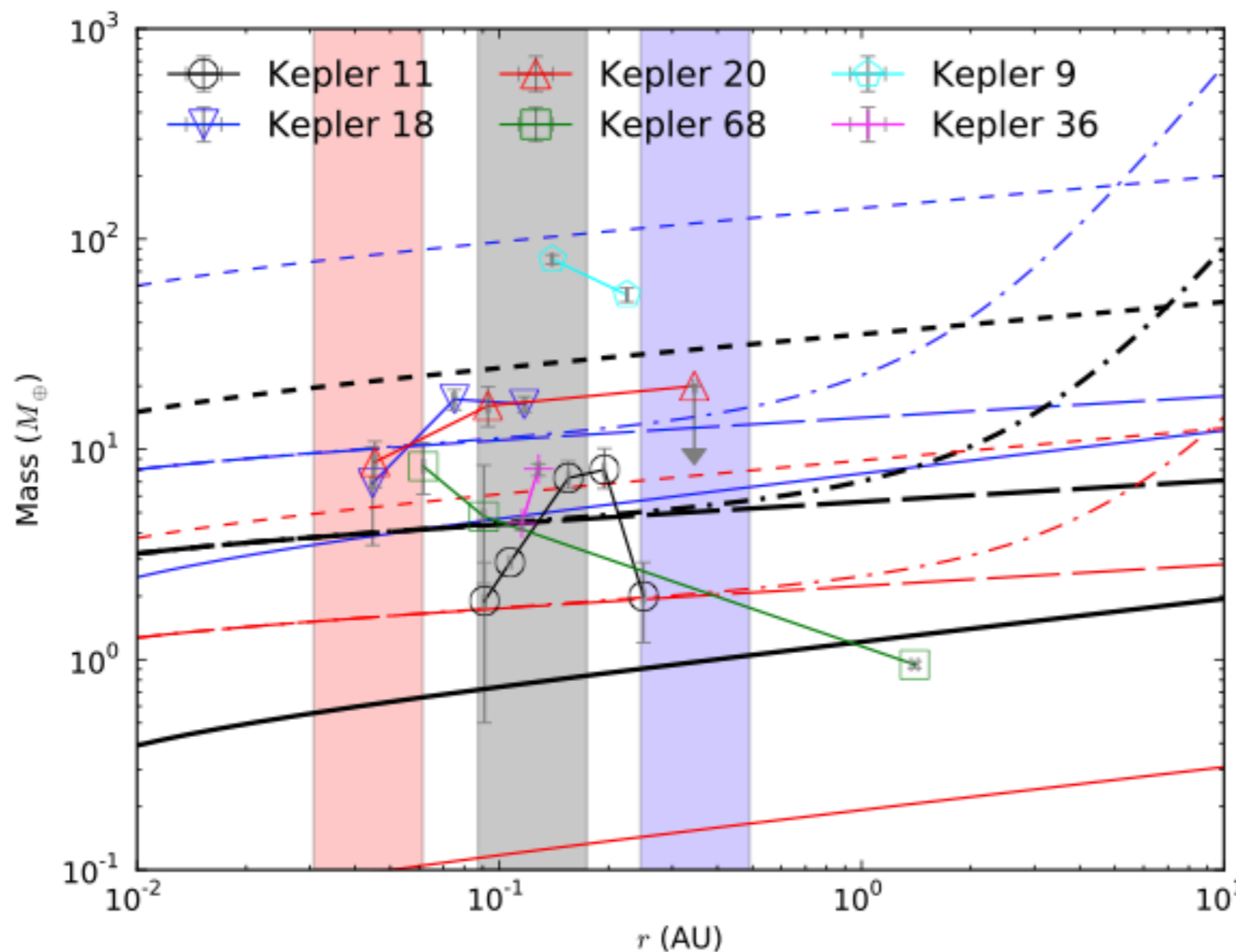

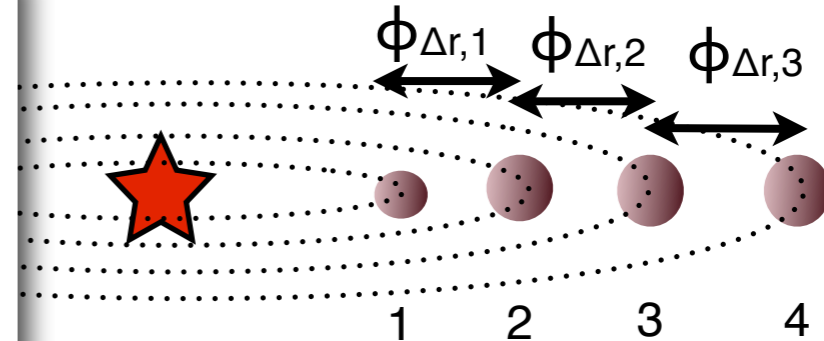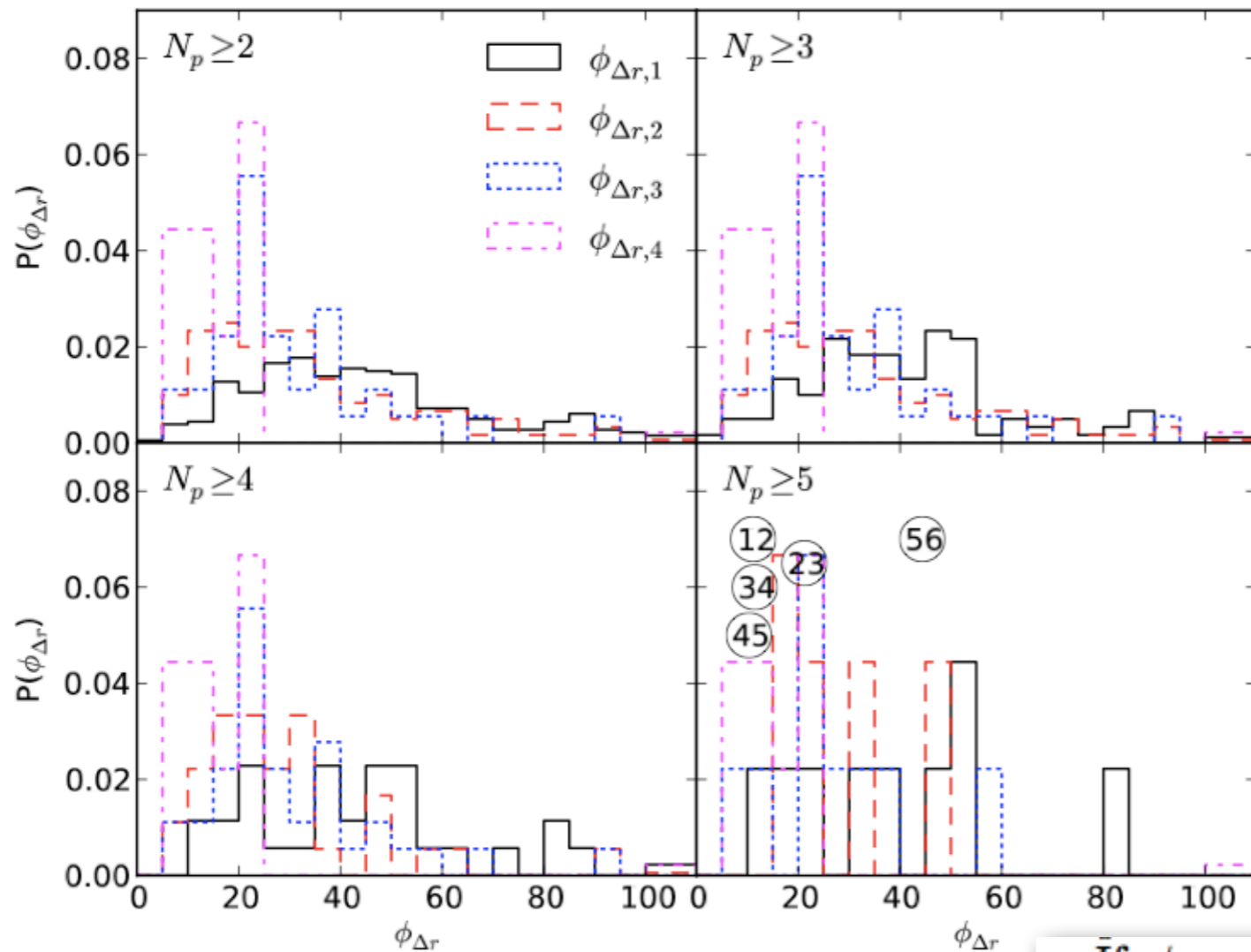Averaging all 6 systems:

$$k_M = 1.0 \pm 2.1$$

Averaging all adjacent pairs:

$$k_M = 0.47 \pm 2.7$$

More masses are needed!

8. Orbital spacings between adjacent planets

Probability distribution of $\phi_{\Delta r}$ for Kepler systems with $N_p \geq 2$ (top-left), 3 (top-right), 4 (bottom-left), and 5 (bottom-right), where $\phi_{\Delta r}$ values for the 6-planet system are shown with inscribed circles.

We measure orbital spacing between adjacent planets normalized by the Hill radius of the inner planet, $\phi_{\Delta r}$, and $\phi_{\Delta r,i}$ uses i to index the inner planet of the pair i and i+1 (planet 1 is closest to the star).

If $\phi_{\Delta r}$ is set by dead zone retreat one may expect greater relative change immediately after formation of the first planet, since this is the first gap-opening episode in the disk. Comparing $\phi_{\Delta r}$ distributions in systems with $N_p \geq 3, 4, 5$ planets (minimal detection bias expected for interior planet locations), indeed $\phi_{\Delta r,1}$ tends to be larger than $\phi_{\Delta r,2}$ and $\phi_{\Delta r,3}$. For $N_p \geq 3$-sample, the KS test gives 9×10^{-5} probability that $(\phi_{\Delta r,1}, \phi_{\Delta r,2})$ are drawn from the same distribution. Equivalent probabilities for $N_p \geq 4$-sample for $(\phi_{\Delta r,1}, \phi_{\Delta r,2})$, $(\phi_{\Delta r,1}, \phi_{\Delta r,3})$, $(\phi_{\Delta r,2}, \phi_{\Delta r,3})$ are 2×10^{-4}, 5×10^{-4}, 0.8, respectively.

| Planet[a] Name	R_{pl} ($R_\oplus$)	M_{pl} ($M_\oplus$)	ρ_{pl} (gcm^{-3})	r (AU)	$\phi_{\Delta r}$[b]	k_M[c] Adjacent Pairs	k_M[d] System
Kepler-9b	9.22 ± 0.8	80 ± 4	0.524 ± 0.132	0.140 ± 0.001	14 ± 1	-0.8	-0.8
Kepler-9c	9.01 ± 0.7	54 ± 4	0.383 ± 0.098	0.225 ± 0.001	-	-	-
Kepler-11b	1.8 ± 0.02	$1.9^{+1.4}_{-1.0}$	$1.77^{+1.29}_{-0.94}$	0.091 ± 0.001	14 ± 5	2.6	0.5
Kepler-11c	$2.87^{+0.01}_{-0.02}$	$2.9^{+2.9}_{-1.6}$	$0.68^{+0.68}_{-0.36}$	0.107 ± 0.001	31 ± 10	2.5	-
Kepler-11d	3.11 ± 0.02	$7.3^{+0.8}_{-1.5}$	$1.33^{+0.15}_{-0.28}$	0.155 ± 0.001	13 ± 2	0.4	-
Kepler-11e	4.18 ± 0.02	$8.0^{+1.5}_{-2.1}$	$0.60^{+0.12}_{-0.16}$	$0.195^{+0.002}_{-0.001}$	14 ± 2	-5.6	-
Kepler-11f	$2.48^{+0.02}_{-0.03}$	$2.0^{+0.8}_{-0.9}$	$0.73^{+0.30}_{-0.34}$	0.250 ± 0.002	-	-	-
Kepler-18b	2.0 ± 0.1	6.9 ± 3.4	4.9 ± 2.4	0.0447 ± 0.0006	35 ± 9	1.8	0.9
Kepler-18c	5.49 ± 0.26	17.3 ± 1.9	0.59 ± 0.07	0.0752 ± 0.0011	21 ± 3	-0.1	-
Kepler-18d	6.98 ± 0.33	16.4 ± 1.4	0.27 ± 0.03	0.1172 ± 0.0017	-	-	-
Kepler-20b	$1.91^{+0.12}_{-0.21}$	$8.7^{+2.1}_{-2.2}$	$6.5^{+2.0}_{-2.7}$	$0.04537^{+0.00054}_{-0.00060}$	49 ± 7	0.8	0.4
Kepler-20c	$3.07^{+0.20}_{-0.31}$	$16.1^{+3.3}_{-3.7}$	$2.91^{+0.85}_{-1.08}$	0.0930 ± 0.0011	104 ± 12	-	-
Kepler-20d	$2.75^{+0.17}_{-0.30}$	< 20	< 4.07	$0.3453^{+0.0041}_{-0.0046}$	-	-	-
Kepler-36b	1.486 ± 0.035	$4.45^{+0.33}_{-0.27}$	$7.46^{+0.74}_{-0.59}$	0.1153 ± 0.0015	7 ± 2	5.6	5.6
Kepler-36c	3.679 ± 0.054	$8.08^{+0.60}_{-0.46}$	$0.89^{+0.07}_{-0.05}$	0.1283 ± 0.0016	-	-	-
Kepler-68b	$2.31^{+0.06}_{-0.09}$	$8.3^{+2.2}_{-2.4}$	$3.32^{+0.86}_{-0.98}$	0.06170 ± 0.00056	23 ± 4	-1.4	-0.6
Kepler-68c	$0.953^{+0.037}_{-0.042}$	$4.8^{+2.5}_{-3.6}$	28^{+13}_{-23}	0.09059 ± 0.00082	878 ± 228	-0.6	-
Kepler-68d	-	0.947 ± 0.035[e]		1.4 ± 0.03	-	-	-

[a]Data for Kepler-9,11,18,20,36,68 from Holman et al. (2010); Lissauer et al. (2013); Cochran et al. (2011); Gautier et al. (2012); Carter et al. (2012); Gilliland et al. (2013), respectively.
[b]$\phi_{\Delta r} = (r_{i+1} - r_i)/R_{H,i}$.
[c]$M_{pl} \propto r^{k_M}$ fitted for adjacent pairs.
[d]$M_{pl} \propto r^{k_M}$ fitted for whole system.
[e]Radial velocity measurement of $M_{pl} \sin i$.
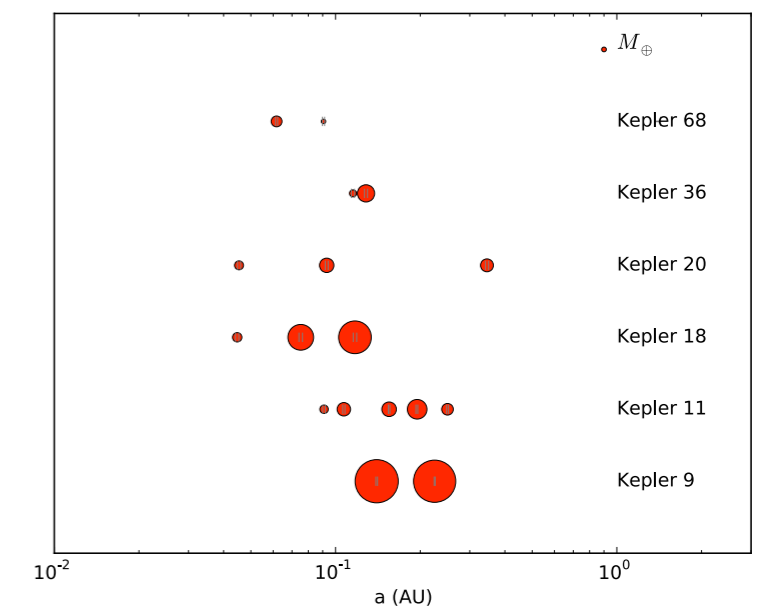
10. Conclusions

Inside-Out Planet Formation: radial drift of cm-m sized solids by gas drag is fast and leads to build up of a massive "pebble" ring at a location of a local pressure maximum. This location is likely to be the inner boundary of the dead zone. Planet formation occurs in this ring, perhaps via gravitational instability. The planet mass may grow until gap-opening, which then causes retreat of the dead zone inner boundary. A new pebble ring forms, slightly further out, and the process repeats. Or the planet Type I migrates inwards, allowing a new ring and planet to form behind it at the fixed dead zone inner boundary.

Features of this model:
- The radial drift of pebbles (part of the "meter-sized barrier" for planet formation) helps direct solids to the inner region for sequential planet formation.
- This process can create ~1-10$M_{\oplus}$ planets on tightly-packed orbits close to the host star, starting from typical protoplanetary disk properties.
- It predicts relatively flat scalings of planetary mass with orbital radius, consistent with observed systems (for the scenario that assumes subsequent migration is negligible).
- Planetary orbital spacings should be >~3 Hill radii of the inner planet of the pair, and the spacing from first to second planet may be relatively larger than subsequent spacings, as is observed.

Next steps:
- Calculation of pebble formation rate for more realistic model of global evolution of pebble population in the disk.
- Numerical simulation of the pebble-dominated ring formation (i.e. Σ_p ~10 Σ_g) and planet formation from such conditions.
- Numerical simulation of dead zone inner boundary evolution.

UF | Astronomy

11. References

Armitage, P. J. 2007, arXiv:astro-ph/0701485
Batalha, N. M. et al. 2013, ApJS, 204, 24
Carter, J. A., Agol, E., Chaplin, W. J. et al. 2012, Science, 337, 556
Chatterjee, S. & Tan, J. C. 2013, arXiv:1306.0576
Chiang, E. & Laughlin, G. 2013, MNRAS, 431, 3444
Cochran, W. D., Fabrycky, D. C., Torres, G. et al. 2011, ApJS, 197, 7
Dzyurkevich, N. et al. 2010, ApJ, 765, 114
Fabrycky et al. 2012).
Fang, J. & Margot, J. L. 2012, ApJ, 761, 92
Gautier, III, T. N., Charbonneau, D., Rowe, J. F. et al. 2012, ApJ, 749, 15
Gilliland, R. L., Marcy, G. W., Rowe, J. F. et al. 2013, ApJ, 766, 40
Hansen, B. & Murray, N. 2012, ApJ, 751, 158
Hansen, B. & Murray, N. 2013, arXiv:1301.7431
Holman, M. J., Fabrycky, D. C., Ragozzine, D. et al. 2010, Science, 330, 51
Kley, W. & Nelson, R. P. 2012, ARA&A, 50, 211
Lissauer, J. J. 1987, Icarus, 69, 249
Lissauer, J. J., Ragozzine, D., Fabrycky, D. C. et al. 2011, ApJS, 197, 8
Lissauer, J. J., Jontof-Hutter, D., Rowe, J. F. et al. 2013, arXiv:1303.0227
Zhu, Z., Stone, J. M., & Rafikov, R. R. 2013, ApJ, 768, 143